

# Novel force field of [Bmim][Nf<sub>2</sub>T] and its transferability in a mixture with water.

Raúl Fuentes-Azcatl  
 rfuentes@ifuap.buap.mx<sup>1</sup> and Minerva González-Melchor  
 minerva@ifuap.buap.mx<sup>2</sup>

<sup>1</sup>Instituto de Física "Luis Rivera Terrazas", Benemérita Universidad Autónoma de Puebla, Apdo. Postal J-48, Puebla, 72570, México,

## Abstract

In this work, a new force field is presented for the ionic liquid 1-butyl-3-methylimidazolium - bis(trifluoromethylsulfonyl)imide, [Bmim][Nf<sub>2</sub>T]. As a part of the  $\epsilon$  force field, the acronym IL/ $\epsilon$  is used to refer to this ionic liquid. This new force field reproduces the dielectric constant, the density, and the enthalpy of vaporization, with an error of less than 3%, being possible to generate new force fields for ionic liquids, based on the flexibility of the molecule. In addition, a study of the [Bmim][Nf<sub>2</sub>T]-H<sub>2</sub>O mixture is performed from pure IL to pure water, passing through various concentrations.

## I. Introduction

The study of ionic liquids (IL) has been extensively analyzed and reported by experimental techniques with the expectation that they could be applied as green solvents in the engineering of chemical reactions.<sup>1</sup> Computer simulation methods and theoretical approaches have been widely used for studies in liquid phase of these systems<sup>2-4</sup> and mixed with polar and non-polar solvents, where a critical point of the liquid-liquid equilibrium at ambient temperature has been observed.<sup>5,6</sup>

In computational theoretical chemistry, there is a wide variety of force fields(FF): from those where molecules are described by all their atoms to those that consider a coarse grain scheme and define a characteristic group of various atoms into a single pseudoatom, which reduces the degrees of freedom and speed up the calculations.<sup>7</sup>

[Bmim][Nf<sub>2</sub>T] is important because it is known to be non-toxic, so it can be applied in metabolite recovery, environmental biotechnology, and biosynthesis of high-value chemicals.<sup>8,9,11</sup> Toxicity studies of IL (acute toxicity assays) are usually based on bioluminescence using microorganisms such as *Vibrio fischeri* or *Photobacterium phosphoreum*,<sup>12,13</sup> so, an adequate study of the mixtures with water is important. The [Bmim][Nf<sub>2</sub>T] is also relevant

for those applications where ILs are employed in the form of thin films supported on solid surfaces, such as in microelectromechanical or microelectronic devices.<sup>14</sup>

After analyzing various models of IL's, it can be concluded that the available FFs do not reproduce all the experimental data, although a large percentage reproduces the density,<sup>7</sup> the values produced for other properties are very dispersed and show large differences with respect to the experimental data. In the work of Acevedo et al.,<sup>15</sup> the charges of a previously proposed FF<sup>16</sup> were reparameterized with a factor of 0.8. Although various properties were improved, they are still far from the experimental data; here we will present this comparison.

Theoretical-computational calculations, specifically those carried out with molecular simulation methods, are currently an important route to understand the role played by molecular interactions on thermodynamic properties and thus, to obtain reliable data on the dynamic and structural properties of non-polarizable liquids. The FF of polar and nonpolar liquids are typically developed by combining electronic structure and molecular simulation calculations to obtain molecular geometries, partial charges of atoms and parameters to reproduce liquid properties, but they also include potentials that give freedom to describe bonds, angles and dihedrals, a procedure that is not uniquely defined.

The remainder of the paper goes as follows: In Section II, the models are introduced. Section III shows the simulation details; in Section IV, the results are analysed, and finally, conclusions are presented in Section V.

## II. Models

The intramolecular energy of [Bmim][Nf<sub>2</sub>T] ionic liquid is evaluated as the sum of contributions due to harmonic bond stretching, angle bending terms and a cosine series for torsional energetics. The non-bonded interactions are described by Coulomb and Lennard-Jones (LJ) potentials. So, the FF parameters are the force constants,  $k_r$  and  $k_\theta$ , the equilibrium bond and angle values,  $r_0$  and  $\theta_0$ , respectively, and the Fourier coefficients  $V$ 's for the torsional energetics function of the angle  $\phi$ , all contained in the following equations,

$$\sum_{bonds} = \sum_i k_{b,i} (r_i - r_{0,i})^2 \quad (\text{S.1})$$

$$\sum_{angles} = \sum_i k_{\theta,i} (\theta_i - \theta_{0,i})^2 \quad (\text{S.2})$$

$$\sum_{torsion} = \sum_i \left[ \frac{1}{2} V_{1,i} (1 + \cos\phi) + \frac{1}{2} V_{2,i} (1 - \cos 2\phi) + \frac{1}{2} V_{3,i} (1 + \cos 3\phi) + \frac{1}{2} V_{4,i} (1 - \cos 4\phi) \right]. \quad (\text{S.3})$$

For the intermolecular potential between two molecules, the LJ and Coulomb interactions of non-polarizable models are used,

$$u(r) = 4\epsilon_{\alpha\beta} \left[ \left( \frac{\sigma_{\alpha\beta}}{r} \right)^{12} - \left( \frac{\sigma_{\alpha\beta}}{r} \right)^6 \right] + \frac{1}{4\pi\epsilon_0} \frac{q_\alpha q_\beta}{r} \quad (\text{S.4})$$

where  $r$  is the distance between sites  $\alpha$  and  $\beta$ ,  $q_\alpha$  is the electric charge of site  $\alpha$ ,  $\epsilon_0$  is the permittivity of vacuum,  $\epsilon_{\alpha\beta}$  is the LJ energy scale, and  $\sigma_{\alpha\beta}$  is the repulsive diameter for an  $\alpha - \beta$  pair. The cross interactions between unlike atoms are obtained using the Lorentz-Berthelot mixing rules,

$$\sigma_{\alpha\beta} = \left( \frac{\sigma_{\alpha\alpha} + \sigma_{\beta\beta}}{2} \right); \quad \epsilon_{\alpha\beta} = (\epsilon_{\alpha\alpha}\epsilon_{\beta\beta})^{1/2}. \quad (\text{S.5})$$

The new force field  $\Pi/\epsilon$  was obtained by changing the angular constants of the harmonic potential  $k_\theta$ . This is because the intramolecular interaction of the atoms has a component due to a restrictive force in their angular movement, and increasing it causes the restrictive force to decrease and atoms to vibrate more. If  $k_\theta$  decreases in order to have a restrictive movement, it is enough to improve the density at various temperatures and reproduce the  $\Delta H$  at room temperature, as will be reported in the results of this work. Although there is freedom in the angle between the atoms of the anions and cations, it was restricted by 20% with respect to that reported by Sambasivarao et al.<sup>16</sup> This FF is all atom, and with the new parameters  $k_\theta$ , the calculated properties are in agreement with the aforementioned experimental data. The value of 20% was found after analyzing a large number of  $k_\theta$  values. We also studied the harmonic potential of the bonds, but it was noted that there was not a better description of the experimental data when  $k_r$  was modified; therefore, in this work only the constants  $k_\theta$  were modified.

### III. Simulation details

The computational calculations were carried out by solving the equations of motion of particles by means of molecular dynamics (MD) simulations on the liquid phase. The simulations were performed using the isothermal-isobaric (NpT) ensemble<sup>17</sup> to obtain the density, the dielectric constant, the self-diffusion coefficient and the heat of vaporization of the system; for this purpose, the GROMACS package was used.<sup>18</sup> The molecules are randomly located in the simulation cell divided in each axis into slices of similar proportions, which generates planes perpendicular to each axis, and at the intersections of these planes, a molecule is placed according to its center of mass. This procedure is done with home-made programs. A total of 500 molecules (250 cations and 250 anions) were used in the simulations of the IL and 864 for the water-IL solution. The equations of motion were solved using the leapfrog algorithm with a time step of 1 fs. Periodic boundary conditions were used in the directions, and the bond distances were kept rigid with the LINCS procedure,<sup>19</sup> when necessary. The cutoff distance was equal to 1.0 nm for both the real part of the Coulomb potential and the LJ interactions; in addition, analytical long-range corrections were applied for the second one. The PME method<sup>20</sup> was applied to evaluate the reciprocal contribution with a grid of 0.34 nm for the reciprocal vectors with a spline of order 4. The Nosé–Hoover thermostat and Parrinello–Rahman barostat were applied with coupling times of 0.6 and 1.0 ps, respectively. The average properties were obtained after production runs of 50 ns, and the time to equilibrate the initial system in the liquid phase was 1 ns.

The surface tension was obtained from a NVT simulation in which a parallelepiped cell was used, with  $L_x = L_y = 13.8$  nm and  $L_z = 3 L_x$  to avoid finite effects,<sup>21,22</sup> containing 5324 molecules. Periodic boundary conditions were applied in all directions. The molecules are initially allocated in a liquid slab surrounded by vacuum with two symmetrical interfaces. The average components of the pressure tensor were obtained for 30 ns after an equilibration period of 5 ns. The densities of the two phases were extracted from the statistical averages of the liquid and vapor limits of the density profiles.<sup>23</sup> The corresponding surface tension  $\gamma$  on the planar interface was calculated from its mechanical definition,<sup>23</sup> according to

$$\gamma = 0.5L_z[\langle P_{zz} \rangle - 0.5(\langle P_{xx} \rangle + \langle P_{yy} \rangle)], \quad (\text{S.6})$$

where  $L_z$  is the length of the simulation cell in the longest direction and  $P_{\alpha\alpha}$  ( $\alpha = x, y, z$ ) are the diagonal components of the pressure tensor. The factor 0.5 outside the squared brackets takes into account the two symmetrical interfaces in the system.

## IV. Results

### A. IL/ $\epsilon$

The new force field was obtained from a previous proposal by Canongia et al.<sup>26,27</sup> by changing the constant  $k_\theta$  of the angular harmonic potential. Such function in the intramolecular part models the restrictive force in the angular movement of molecules. An increase in  $k_\theta$  causes an increase in the force; the frequency of oscillation also increases, and therefore, molecules vibrate more. So, by decreasing  $k_\theta$  in order to relax the restrictive force, it can be enough to produce changes in the properties, improving the density, the dielectric constant, and the enthalpy of vaporization  $\Delta H_{vap}$  at different temperatures. Although there is freedom in choosing the angle between the atoms of the anions and cations, when it was restricted by 20% with respect to that reported by Canongia et al.,<sup>26,27</sup> the agreement between the aforementioned properties and the experimental data improved. The value of 20% was found after analyzing a large number of  $k_\theta$ -values. In addition, the harmonic potential of the bonds was studied too, however, it was noted that modifications to  $k_r$  did not produce a better description of the properties. Therefore, it was decided to only modify the constant  $k_\theta$ . This method, identified as the  $\text{CO}_2/\epsilon$ ,<sup>25</sup> has been previously used to parameterize the  $\text{CO}_2$  molecule, improving the properties already mentioned when contrasting them with the experimental data.

#### 1. Density, $\rho$

The density of the ionic liquid [Bmim][Nf<sub>2</sub>T] has been widely studied and reported by various research groups, with different approaches to molecules, from those that describe all the atoms to those that, in a pseudo-atom, include the contribution of a set of atoms, mainly hydrogens, which are taken into account in a united atom.<sup>7</sup>

In this paper, we will compare our new IL/ $\epsilon$  model with the all-atom models of Doherty et al.<sup>15</sup> and Sambasivarao et al.,<sup>16</sup> and with the newly parameterized united atom model

developed by Martínez-Jiménez et al.<sup>7</sup> The calculated density is shown in figure 1, where an excellent agreement with experimental data is observed for all temperatures.

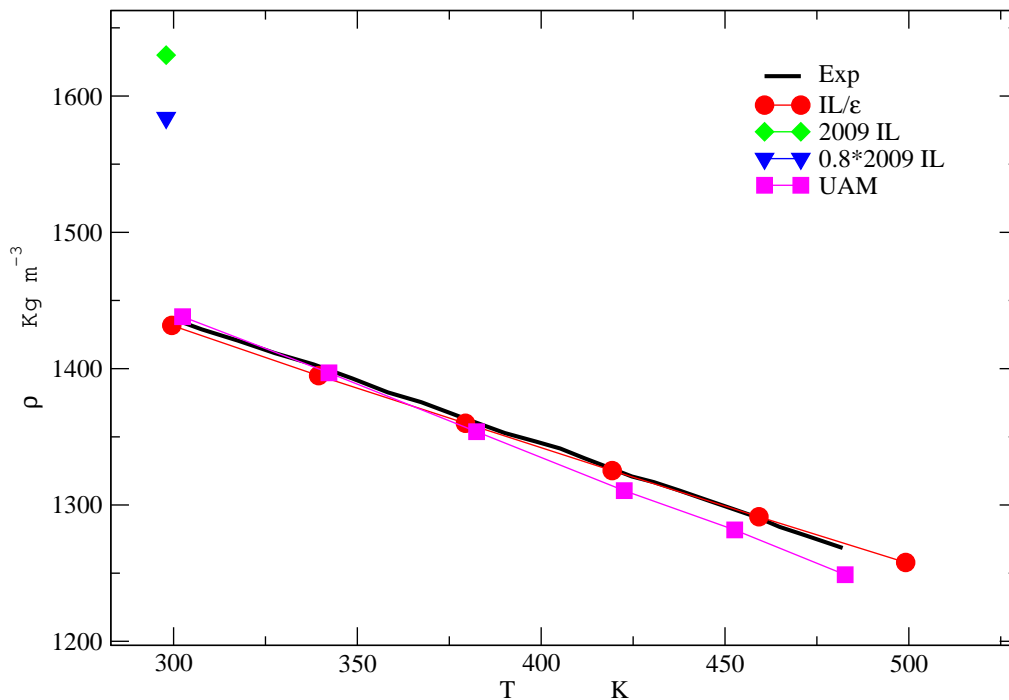


Figure 1: Density of the system [Bmim][Nf<sub>2</sub>T] at different temperatures. Black triangles are the experimental data.<sup>30</sup> The red circles are the results of IL/ε, the blue triangle is reported by Doherty et al.,<sup>15</sup> the green diamond is reported by Sambasivarao et al.,<sup>16</sup> and the magenta square by Martínez-Jiménez et al.<sup>7</sup>

## 2. Heat of vaporization, $\Delta H_{vap}$

An important characteristic of ionic liquids is the vaporization enthalpy, its magnitude is generally greater than that of other molecular liquids due to the strong electrostatic interactions between the ions. Reproducing heats of vaporization,  $\Delta H_{vap}$ , is particularly important as it serves as an indicator of the average intermolecular interactions.

The calculation of  $\Delta H_{vap}$  is obtained by means of the energetic difference between the liquid phase and the gas phase,

$$\Delta H_{vap} = \Delta H_{gas} - \Delta H_{liq}, \quad (\text{S.7})$$

TABLE S 1: Calculated and Experimental Heat of Vaporization (kJ/mol) at 298 K.

Exp.	2009IL	% error	0.8*2009 IL	% error	UAM	% error	IL/ $\epsilon$	% error
134.7	190.4	41.3	154.8	14.9	50.68	62.4	134.1	0.4

which can be written as:

$$\Delta H_{vap} = E_{total}(gas) - E_{total}(liq) + RT. \quad (S.8)$$

Experimental data has shown that ionic liquids go into the vapor phase as an ion pair,<sup>28,32</sup> then the energy  $E_{total}(gas)$  is calculated using a single ion pair and  $E_{total}(liquid)$  is the corresponding value in the condensed phase. In the simulation we have obtained the PV term and it is used in place of RT term.

The parameterization carried out by Doherty et al,<sup>15</sup> by reducing the general charge of the ionic liquid molecules reduced the error by 26.4%, but even so the error is large. With the new force field the error was reduced to 0.4% , which basically equals the calculated  $\Delta H_{vap}$  to its experimental value, as shown in Table 1.

### 3. Surface tension, $\gamma$

In the study carried out by Doherty et al,<sup>15</sup> the reproduction of the surface tension improved: the value they reported has an error of 29.23%. In this work that data is compared with the new force field IL/ $\epsilon$  value.

The calculation of the surface tension in ionic liquids is fundamental due to its nature, since essentially, the tangential components of the pressure define it. In general, the surface tension is high within a wide range of temperatures. Another property related to this phenomenon is the vapor pressure, which is very low.

In the figure 2, the results of the new force field IL/ $\epsilon$  are shown. The surface tension decreases as the temperature increases, the IL/ $\epsilon$  force field reproduces the experimental trend but moves away from those data in a proportion of 30 % at 298 K and 19.6 % at 425 K while the vapor pressure remains low, as data in table 2 shows, indicating strong cohesion between the ions and, as consequence, a low volatility.

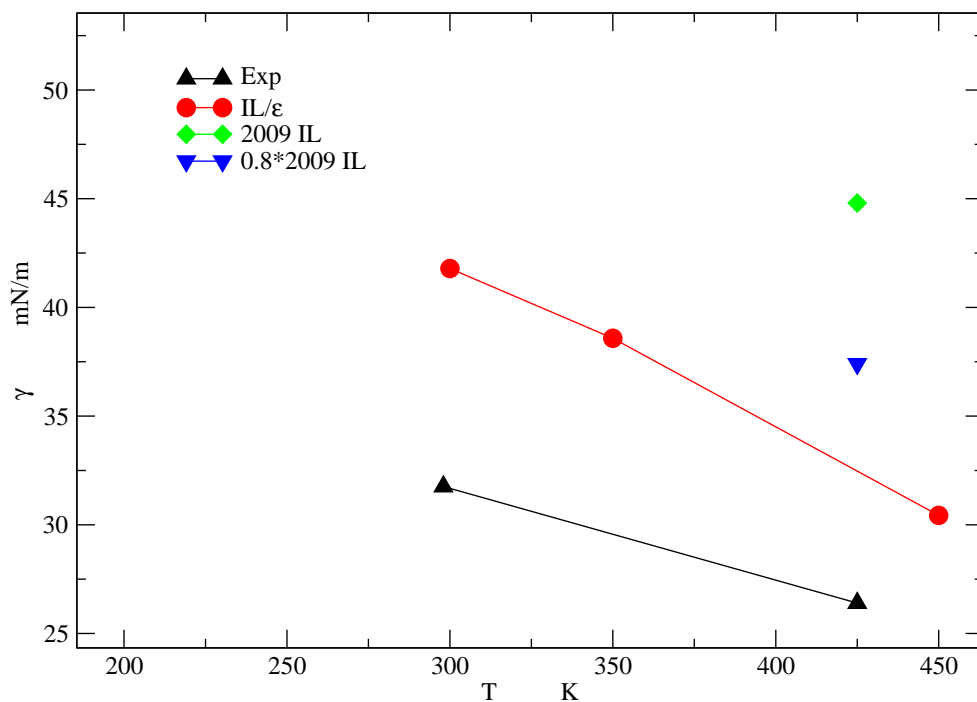


Figure 2: The surface tension of the system [bmim] [Tf2 N] at different temperatures. Black triangles are the experimental data.<sup>30</sup> the red circles are the result of IL/ $\epsilon$ , the blue triangle is reported by Doherty et al<sup>15</sup>, the green is reported by Sambasivarao et al<sup>16</sup>

TABLE S 2: Absolute vapor pressure at different temperatures of the IL/ $\epsilon$ .

Temp. K	$ P_{vap} _{DM}$ bar	$P_{vapExp}$ bar
300	0.146	-
350	0.142	-
450	0.094	7.1e-8

#### 4. Dielectric constant, $\epsilon$ .

Ionic liquids are charged molecules and inherent to their study, an analysis of electrical behavior must be considered. A property governed by the interactions produced by the charges and their positions in space is the dielectric constant, which is calculated through the fluctuations in the total dipole moment of the system,<sup>24</sup>

$$\epsilon = 1 + \frac{4}{3k_B T V} (\langle M^2 \rangle - \langle M \rangle^2), \quad (\text{S.9})$$

where  $k_B$  is the Boltzmann constant and  $T$  is the absolute temperature. The dielectric constant was obtained from simulations of 55 ns using the isotropic NPT ensemble, which are long compared to simulation times required to calculate other properties, such as the surface tension. The proper evaluation of the dielectric constant needs long simulations to ensure an average dipole moment of the system around zero<sup>29</sup> and the convergence of the property with time.



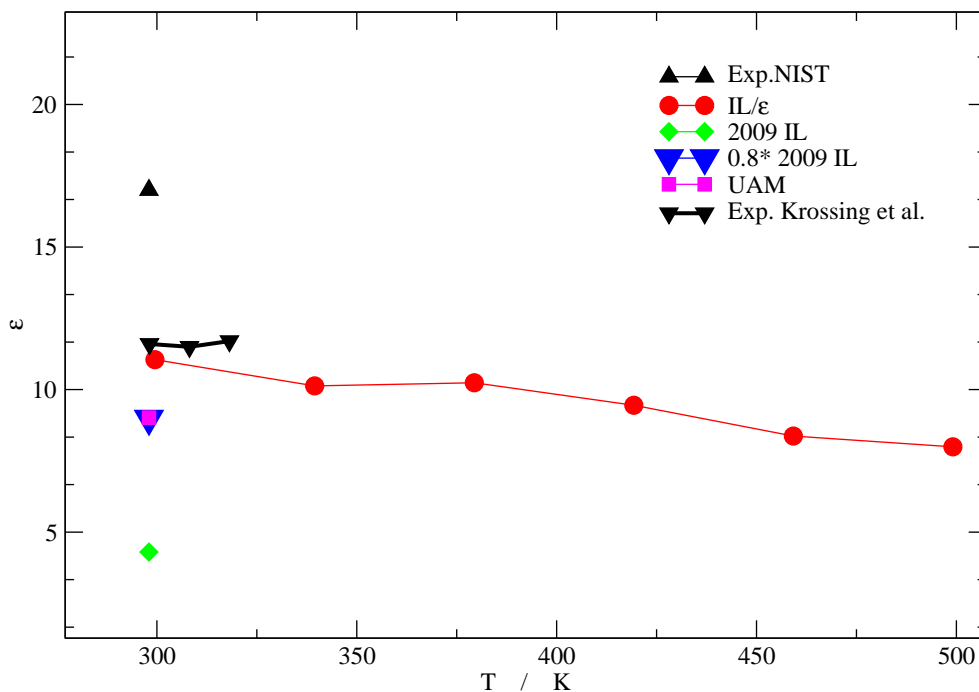


Figure 3: Dielectric constant of the system [Bmim][Tf2N] at different temperatures. Black triangle up is the experimental data taken from NIST database,<sup>33</sup> black triangle down is the experimental data reported by Crossing et al.<sup>42</sup> the red circles are the result of IL/ $\epsilon$ , the blue triangle by Doherty et al,<sup>15</sup> the green diamond by Sambasivarao et al<sup>16</sup>, magenta square by Martínez-Jiménez et al,<sup>7</sup> all were calculated in this work

The results of the dielectric constant, obtained from the molecular dynamic calculations, are shown in the figure 3. All the force fields studied here were compared by evaluating  $\epsilon$  at 300 K and 1 bar. There is an important difference between the values reported at the NIST database<sup>33</sup> and those reported in the work of Crossing et al;<sup>42</sup> taking into account the values of Crossing and coworkers, the 2009IL is 63.2% far from the experimental data, the 0.8\*2009IL is 22.4% far equal to the UAM FF while the result produced by the IL/ $\epsilon$  FF has a difference of 5%. Although the dielectric constant is low in all FFs, the value here reported and calculated using the new IL/ $\epsilon$  model is the closest to the experimental data. From the references found and analyzed, we noted that the dielectric constant is not reported. Since  $\epsilon$  is a very important property due to the nature of the Coulombic interactions in these fluids, our work contributes filling this gap in the description of IL's.

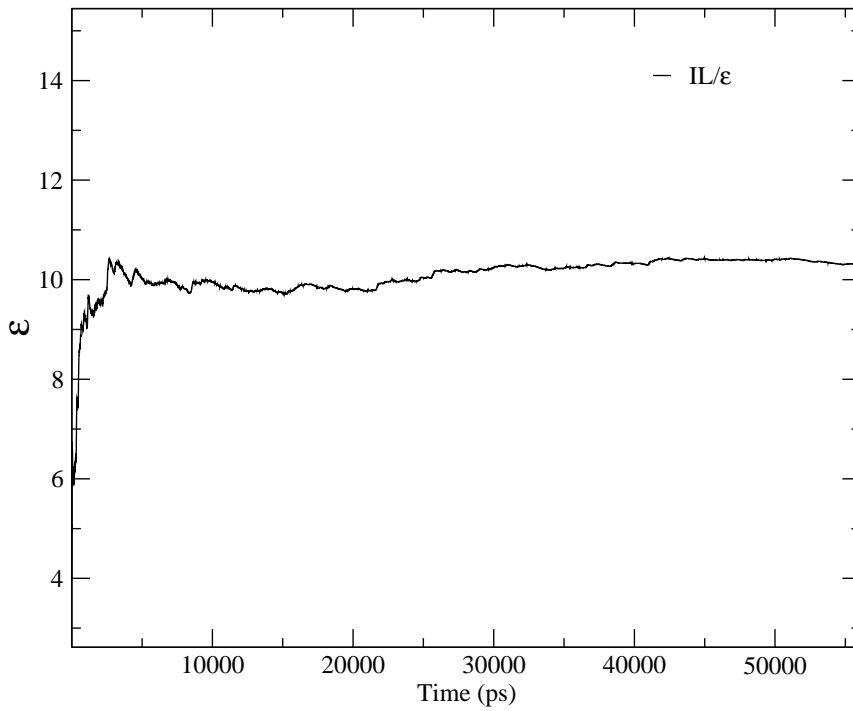


Figure 4: Dielectric constant of IL/ $\epsilon$ . evaluation of the dielectric constant after 55 nanoseconds.

The figure 4 shows the calculated dielectric constant in time to 55 nanoseconds. As observed, this long simulation time is required to reach the stability shown because within the first 30 ns the value fluctuates, generating errors of 10% or more.

## 5. Self diffusion coefficient, $D$ .

The self diffusion coefficients of the cation, D+, and anion, D-, were determined using the Einstein relation, which connects the mean-square displacement (MSD) to the self diffusion in the limit of long times, through

$$D = \lim_{t \rightarrow \infty} \frac{1}{6t} \langle \sum_{i=1}^N [\vec{r}_i(t) - \vec{r}_i(0)]^2 \rangle, \quad (\text{S.10})$$

where, in the calculations, we used the position of the center of mass of each ion,  $\vec{r}_i$ .<sup>29</sup>

Typically, the absolute values of the ion diffusion constants are 2 orders of magnitude smaller than those of water,<sup>36</sup> i.e.,  $10^{-11}$  m<sup>2</sup>/s. Figures 5 and 6 show the data obtained for D+ and D- with the new  $\Pi/\epsilon$  FF, and those reported by Doherty et al,<sup>15</sup> Sambasivarao et al<sup>16</sup> and Martínez-Jiménez et al.<sup>7</sup> The later is the one that best reproduces the experimental value, which is not a surprise since it was an objective property in the reparameterization of the UAM FF, as well as the experimental density.<sup>7</sup>

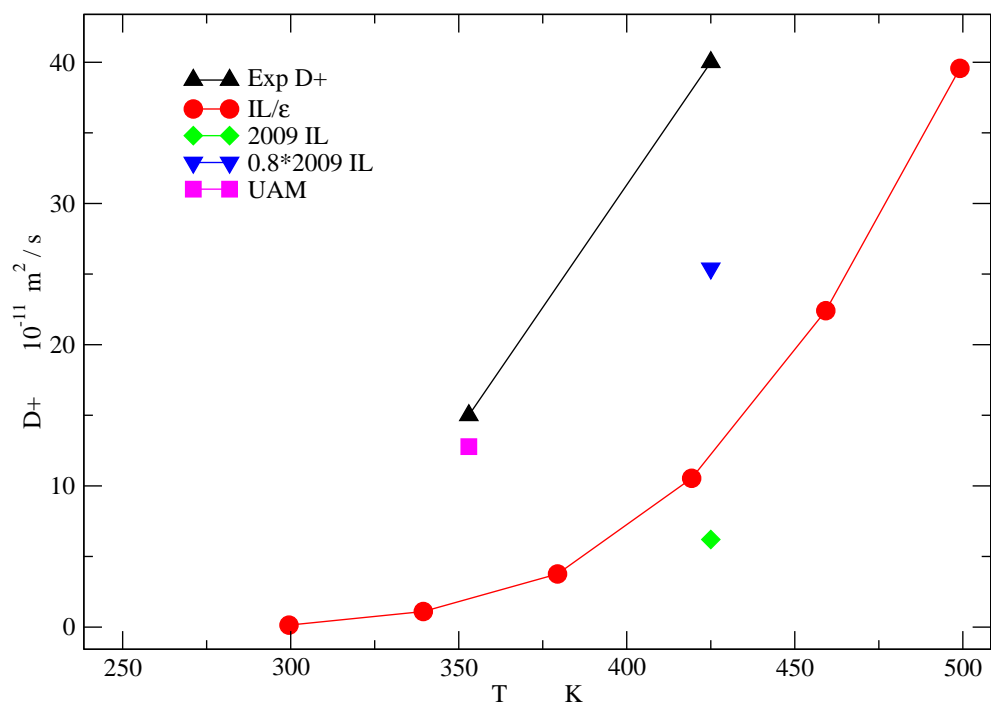


Figure 5: self diffusion coefficient of cation in the system [bmim] [Tf<sub>2</sub>N] at different temperatures. Black triangles are the experimental data. the red circles are the result of IL/ $\epsilon$ , the blue down triangle is reported by Doherty et al<sup>15</sup>, the green diamond is reported by Sambasivarao et al<sup>16</sup> and magenta square was reported by [Martínez-Jiménez et al.<sup>7</sup>](#)

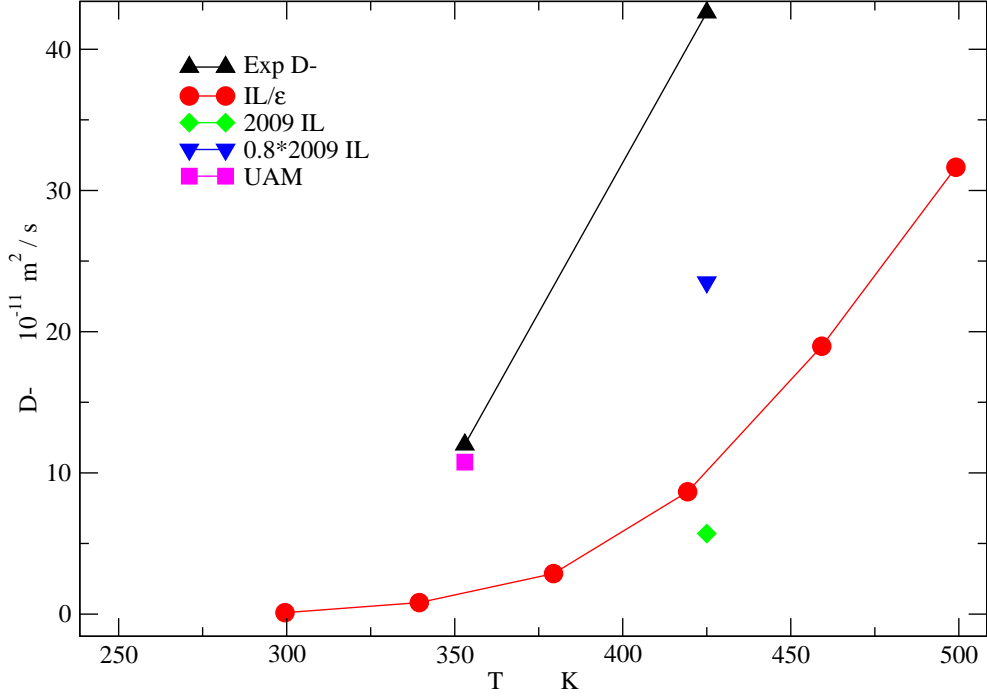


Figure 6: self diffusion coefficient of anion in the system [bmin] [Tf2N] at different temperatures. Black triangles are the experimental data. the red circles are the result of IL/ $\epsilon$ , the blue down triangle is reported by Doherty et al<sup>15</sup>, the green diamond is reported by Sambasivarao et al<sup>16</sup> and magenta square was reported by Martínez-Jiménez et al.<sup>7</sup>

## 6. Isothermal compressibility, $k_T$ .

The evaluation of how pressure affects density at constant temperature is determined by calculating the isothermal compressibility,  $k_T$ . The calculation of this property is done by means of the fluctuations in the volume during the simulation in the NPT ensemble, as shown in the equation S.11

$$k_T = \frac{1}{\rho} \left( \frac{\partial \rho}{\partial P} \right)_T = \frac{\langle V^2 \rangle - \langle V \rangle^2}{k_B T \langle V \rangle} \quad (\text{S.11})$$

The data obtained in this work are shown in figure 7. The value produced by the 2009IL FF and that of the 0.8\*2009IL FF are far from the experimental value whereas the UAM FF

produces a value with an error of 31% greater the experimental value at 300 K and 1 bar while the new IL/ $\epsilon$  FF has an error of 172% at those conditions. Several values of  $k_T$  were calculated with the new FF IL/ $\epsilon$  to analyze its behavior when the temperature rises. We see that it decreases and in general keeps a behavior with little change, while the experiments indicate that it must increase, suggesting that in this new FF the attractive interactions or hydrogen bonding are overestimated and the system do not expand as temperature rises. For most simple liquids, the compressibility decreases with decrease in temperature as the volume fluctuation decreases, whereas in our case the behavior is similar to water below about 320 K, i.e., compressibility is higher when temperature decreases.

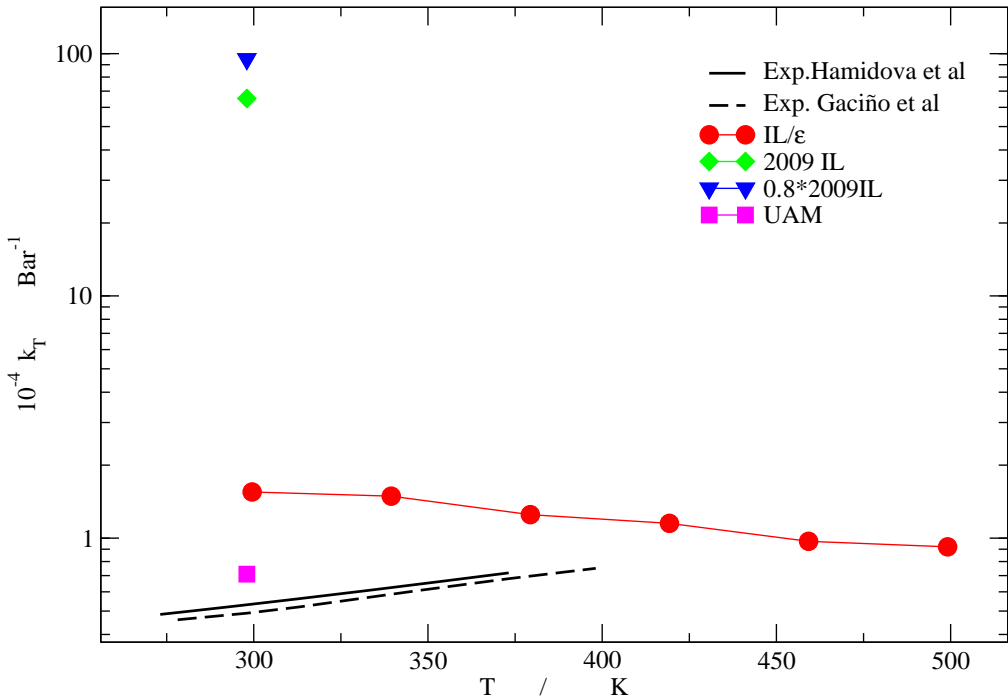


Figure 7: Isothermal compressibility of the system [Bmim] [Tf2N] at different temperatures. Black line reported by Hamidova et al<sup>30</sup> and black dash line reported by Gaciño et al<sup>31</sup> are the experimental data, the red circles are the result of IL/ $\epsilon$ , the blue down triangle by Doherty et al,<sup>15</sup> the green diamond by Sambasivarao et al,<sup>16</sup> magenta square by Martínez-Jiménez et al<sup>7</sup> all were calculated in this work.

## B. Mixture of IL/ $\epsilon$ - H<sub>2</sub>O.

By reparameterizing the [Bmim][Nf<sub>2</sub>T] system, the performance of this new FF is evaluated in a mixture with water, the FBA/ $\epsilon$ <sup>40</sup> flexible 3-sites water model is used, this model improves the reproduction of experimental data at various thermodynamic conditions with respect to other rigid or flexible three sites models with equal interaction potentials.<sup>37</sup> This evaluation process has been carried out successfully in the case of NaCl<sup>38</sup> and KBr,<sup>39</sup> which originates a systematic test for ionic species.

As reported in the work of Fuentes et al<sup>6</sup> with three different water force fields, the reproduction of the thermodynamic properties of the mixture is very similar in low and high concentrations regardless of the water model used, for this reason in this work, only the FAB/ $\epsilon$  model was used, which performs well at the pressure and temperature conditions studied in this work.

### 1. Density, $\rho$ .

A second reason to use the FBA/ $\epsilon$  water model, is because among the three-site models, it is the one that best reproduces the experimental values of density, heat of vaporization, surface tension and dielectric constant.<sup>40</sup> So, these properties were evaluated for the mixture of IL/ $\epsilon$  with H<sub>2</sub>O. The result of the density with respect to the temperature at a pressure of 1 bar can be seen in the figure 8, where the values of the pure substances reproduce the experimental data. It is observed that in the molar fraction of  $X_{H_2O}=3$ , the experimental data is reproduced. Therefore, our results suggest that is highly likely that the experimental data of the mixture will be well reproduced by the new FF.

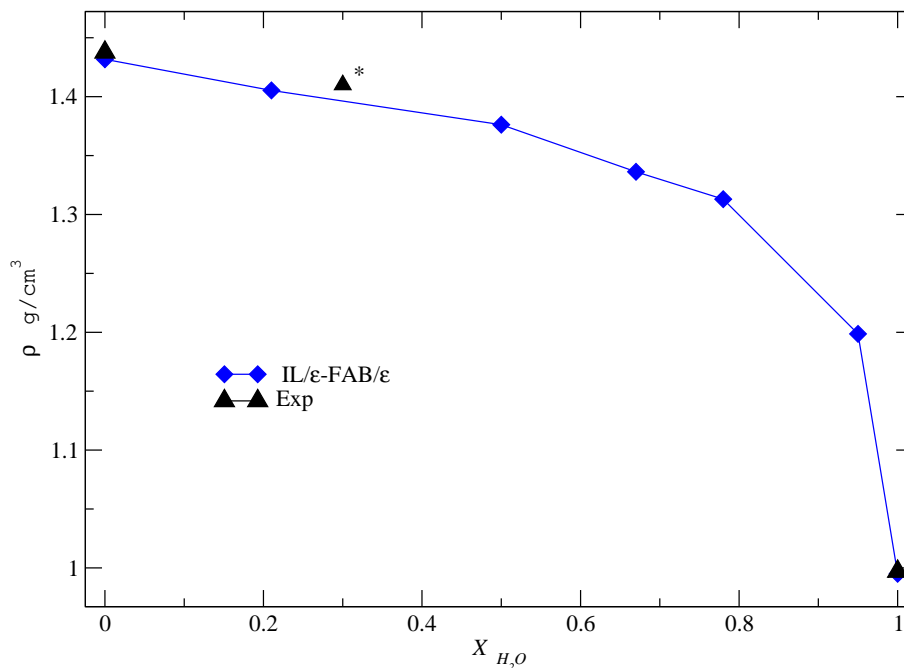


Figure 8: Density of the water–IL solution as a function of the molar fraction of water at 1 bar of pressure. Black triangles are the experimental data,<sup>34</sup> black triangle-asterisk is the experimental data reported by Jacquemin et al. with water-saturated sample,<sup>35</sup> the blue diamonds are the result using FAB/ $\epsilon$  model, all calculated in this work

## 2. Heat of Vaporization, $\Delta H_{vap}$ .

In the experiments carried out by Zaitsau et al<sup>41</sup> they demonstrated the equilibrium of thermal stability and volatility for [Bmim][NTf<sub>2</sub>]. In fact, they made measurements of vapor pressures in a temperature interval large enough for an adequate evaluation of the thermodynamic parameters, such as the change of enthalpy from the gas phase to the liquid phase  $\Delta H_{vap}$ . In the figure 9 it can be seen how both models, the one for the ionic liquid IL/ $\epsilon$  and that of water, the FBA/ $\epsilon$ , reproduce the experimental data with a minimum percentage of error. Then, from calculations at different proportions of water and IL, we calculated the values of  $\Delta H_{vap}$  of the mixture, which maintain a reasonable behavior and adapt well to the range of values of the pure components.



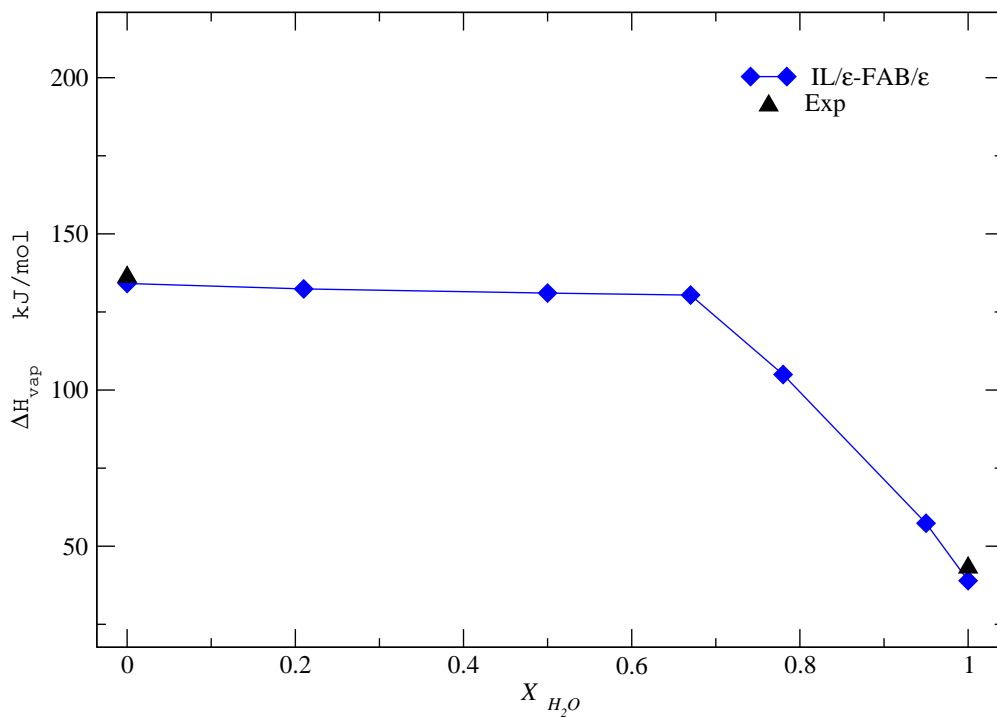


Figure 9:  $\Delta H_{vap}$  of the system with respect to the fraction of water in the solution Il-water. Both at 1 bar of pressure and 300 K of temperature. Black triangles are the experimental data,<sup>41</sup> the blue diamonds are the result using FAB/ $\epsilon$  model, all calculated in this work

### 3. Surface tension, $\gamma$ .

The surface tension of the system when the fraction mol of water increases,  $X_{H_2O}$ , is shown in figure 10. The new FF Il/ $\epsilon$  overestimated the experimental value of the surface tension with an error of 23.8%, but when the mol fraction of water increases, the trend is almost the same until  $X_{H_2O}=0.9$ . At this concentration, the surface tension increased and reach the experimental value of pure water with an error of 3%, indicating that the ionic liquid governs the surface tension up to the limit of  $X_{H_2O}=0.9$ .

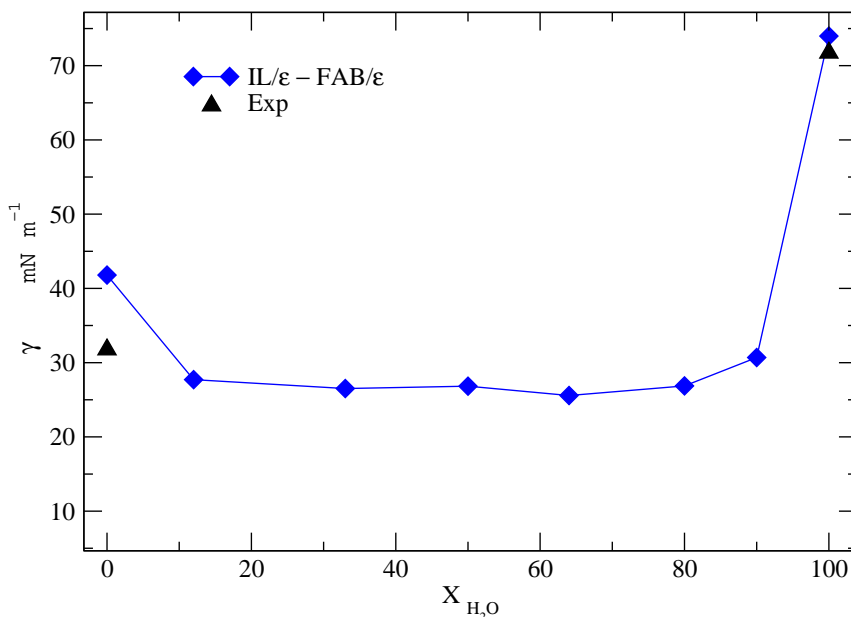


Figure 10: The surface tension of the system with respect to the fraction mol of water in the solution IL-water. Black triangles are the experimental data,<sup>30,33</sup> the blue diamonds are the result using FAB/ $\epsilon$  model with the IL/ $\epsilon$ , all calculated in this work

#### 4. Dielectric constant, $\epsilon$ .

The calculation of the dielectric constant of the system is shown in figure 11. The error the FF IL/ $\epsilon$  carries is 35% respect to the NIST database<sup>33</sup> and 5% respect to that reported by Krossing et al.<sup>42</sup> The FAB/ $\epsilon$  FF of water at these conditions has a 3.8% of error respect to the experimental data, then taking this into account, the values obtained for the mixture have that percentage of error. Even so, the electrostatic interactions generated by the IL govern the behavior of the mixture up to  $X_{H_2O}=0.8$ , where the greater presence of water causes the system to increase the value of  $\epsilon$ , to finally reach a value very close to the experimental one with the error indicated above.

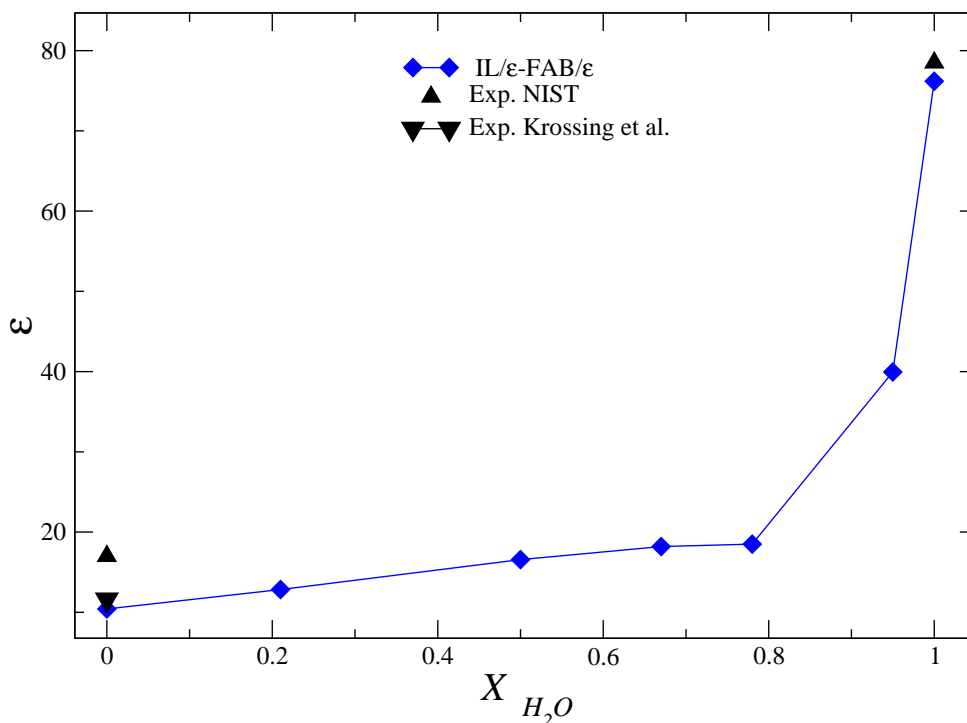


Figure 11: Dielectric constant of the water-IL solution as a function of the molar fraction of water at 1 bar of pressure and 298 K of temperature. Black triangles are the experimental data.<sup>33</sup> The blue diamonds are the result using FAB/ $\epsilon$  model, all calculated in this work

## V. Conclusion

In this work, the ionic liquid [Bmim][Nf<sub>2</sub>T] was reparameterized, which improved the reproduction of density,  $\Delta H_{vap}$ , and the dielectric constant. The isothermal compressibility, self-diffusion coefficient and surface tension are also reported, which improve the reproduction of these properties with respect to the force fields compared here. There are still expectations and challenges to improve the force fields of the ionic liquids and have a better description of the experimental values at different conditions of pressure and temperature. There is also room to predict and eventually improve the values of the properties here reported when the IL's are combined with other molecules. The reported the properties of the mixture of IL and

water, calculated with the new force field at different concentrations, being certain that each model reproduce the experimental properties separately, and obtained a consistent behavior for the values of the mixture. These findings suggest that the predicted properties would be in good agreement with the experimental data. The data here reported for density,  $\Delta H_{vap}$ , surface tension and dielectric constant, leave a broader picture of what the new force fields can reproduce. With force fields capable of reproducing experimental properties with less error, there is greater certainty that they will reproduce values at different thermodynamic states and concentrations where there are still no experimental data.

## VI. Acknowledgements

RFA thanks CONACYT for a postdoctoral fellowship. The authors acknowledge the computer resources and support provided by Laboratorio Nacional de Supercómputo del Sureste de México, CONACYT network of national laboratories. Support from VIEP-BUAP through project CA-191-GOMM (2023) is also acknowledged.

## References

- [1] Badgujar, K. & Bhanage, B. Factors governing dissolution process of lignocellulosic biomass in ionic liquid: Current status, overview and challenges. *Bioresource Technology*. **178** pp. 2-18 (2015), <https://www.sciencedirect.com/science/article/pii/S0960852414013972>
- [2] Pandey, S. Analytical applications of room-temperature ionic liquids: A review of recent efforts. *Analytica Chimica Acta*. **556**, 38-45 (2006), <https://www.sciencedirect.com/science/article/pii/S0003267005010214>, Young Analytical Faculty in Asia
- [3] Canongia Lopes, J., Deschamps, J. & Pádua, A. Modeling Ionic Liquids Using a Systematic All-Atom Force Field. *The Journal Of Physical Chemistry B*. **108**, 2038-2047 (2004,2), <https://doi.org/10.1021/jp0362133>
- [4] Roosen, C., Müller, P. & Greiner, L. Ionic liquids in biotechnology: applications and perspectives for biotransformations. *Applied Microbiology And Biotechnology*. **81**, 607-614 (2008,12), <https://doi.org/10.1007/s00253-008-1730-9>
- [5] Schroer, W., Triolo, A. & Russina, O. Nature of Mesoscopic Organization in Protic Ionic Liquid–Alcohol Mixtures. *The Journal Of Physical Chemistry B*. **120**, 2638-2643 (2016,3), <https://doi.org/10.1021/acs.jpcc.6b01422>
- [6] Fuentes-Azcatl, R., Araujo, G., Lourenço, T., Costa, C., Carneiro, J. & Costa, L. Dielectric behavior of water in [bmim] [Tf<sub>2</sub>N] room-temperature ionic liquid: molecular dynamic study. *Theoretical Chemistry Accounts*. **140**, 125 (2021,8), <https://doi.org/10.1007/s00214-021-02825-x>

- [7] Martínez-Jiménez, M., Serrano-Ocaña, M. & Alejandre, J. United atom model for ionic liquids: UAM-IL. *Journal Of Molecular Liquids*. **329** pp. 115488 (2021), <https://www.sciencedirect.com/science/article/pii/S0167732221002142>
- [8] Quijano, G., Couvert, A., Amrane, A., Darracq, G., Couriol, C., Le Cloirec, P., Paquin, L. & Carrié, D. Toxicity and biodegradability of ionic liquids: New perspectives towards whole-cell biotechnological applications. *Chemical Engineering Journal*. **174**, 27-32 (2011), <https://www.sciencedirect.com/science/article/pii/S1385894711008990>
- [9] R. Muñoz, S. Villaverde, B. Guieysse, & S. Revah, Two-phase partitioning bioreactors for treatment of volatile organic compounds, *Biotechnol. Adv.* **25** (2007) 410-422.
- [10] J.L.E. Morrish, E.T. Brennan, H.C. Dry, & A.J. Daugulis, Enhanced bioproduction of carvone in a two-liquid-phase partitioning bioreactor with a highly hydrophobic biocatalyst, *Biotechnol. Bioeng.* **101** (2008) 768-775.
- [11] J.J. Malinowski, & A.J. Daugulis, The effective approach for recovery of methylsubstituted 1,3-dioxane from aqueous media, *Sep. Sci. Technol.* **37** (2002) 2659-2667.
- [12] A. Romero, A. Santos, J. Tojo, & A. Rodriguez, Toxicity and biodegradability of imidazolium ionic liquids, *J. Hazard. Mater.* **151** (2008) 268-273.
- [13] M.T. Garcia, N. Gathergood, P.J. Scammells, Biodegradable ionic liquids: Part II. Effect of the anion and toxicology, *Green Chem.* **7** (2005) 9-14.
- [14] Bovio, S., Podestá, A., Lenardi, C. & Milani, P. Evidence of Extended Solidlike Layering in [Bmim][NTf<sub>2</sub>] Ionic Liquid Thin Films at Room-Temperature. *The Journal Of Physical Chemistry B*. **113**, 6600-6603 (2009,5), <https://doi.org/10.1021/jp9022234>
- [15] Doherty, B., Zhong, X., Gathiaka, S., Li, B. & Acevedo, O. Revisiting OPLS Force Field Parameters for Ionic Liquid Simulations. *J. Chem. Theory Comput.* **13**, 6131-6145 (2017,12)
- [16] Sambasivarao, S. & Acevedo, O. Development of OPLS-AA Force Field Parameters for 68 Unique Ionic Liquids. *J. Chem. Theory Comput.* **5**, 1038-1050 (2009,4)
- [17] Tuckerman, M. *Statistical mechanics: theory and molecular simulation*. (Oxford university press, 2010).
- [18] Van Der Spoel, D., Lindahl, E., Hess, B., Groenhof, G., Mark, A. & Berendsen, H. GROMACS: fast, flexible, and free. *J Comput Chem.* **26**, 1701-1718 (2005,12).
- [19] Hess, B., Kutzner, C., Spoel, D. & Lindahl, E. GROMACS 4: Algorithms for Highly Efficient, Load-Balanced, and Scalable Molecular Simulation. *J. Chem. Theory Comput.* **4**, 435-447 (2008,3).
- [20] Essmann, U., Perera, L., Berkowitz, M., Darden, T., Lee, H. & Pedersen, L. A smooth particle mesh Ewald method. *jcp.* **103**, 8577-8593 (1995,11).

- [21] Orea, P., López-Lemus, J. & Alejandre, J. Oscillatory surface tension due to finite-size effects. *The Journal Of Chemical Physics*. **123**, 114702 (2005)
- [22] González-Melchor, M., Orea, P., López-Lemus, J., Bresme, F. & Alejandre, J. Stress anisotropy induced by periodic boundary conditions. *The Journal Of Chemical Physics*. **122**, 094503 (2005),
- [23] Alejandre, J., Tildesley, D. & Chapela, G. Molecular dynamics simulation of the orthobaric densities and surface tension of water. *The Journal Of Chemical Physics*. **102**, 4574-4583 (1995),
- [24] Neumann, M. Dipole moment fluctuation formulas in computer simulations of polar systems. *Molecular Physics*. **50**, 841-858 (1983)
- [25] Fuentes-Azcatl, R. & Domínguez, H. Prediction of experimental properties of CO<sub>2</sub>: improving actual force fields. *Journal Of Molecular Modeling*. **25**, 146 (2019,5), <https://doi.org/10.1007/s00894-019-4034-3>
- [26] Canongia Lopes, J. & Pádua, A. Molecular Force Field for Ionic Liquids III: Imidazolium, Pyridinium, and Phosphonium Cations; Chloride, Bromide, and Dicyanamide Anions. *The Journal Of Physical Chemistry B*. **110**, 19586-19592 (2006,10), <https://doi.org/10.1021/jp063901o>
- [27] Canongia Lopes, J., Pádua, A. & Shimizu, K. Molecular Force Field for Ionic Liquids IV: Trialkylimidazolium and Alkoxy carbonyl-Imidazolium Cations; Alkylsulfonate and Alkylsulfate Anions. *The Journal Of Physical Chemistry B*. **112**, 5039-5046 (2008,4), <https://doi.org/10.1021/jp800281e>
- [28] Malberg, F., Hollóczki, O., Thomas, M. & Kirchner, B. En route formation of ion pairs at the ionic liquid–vacuum interface. *Structural Chemistry*. **26**, 1343-1349 (2015,12), <https://doi.org/10.1007/s11224-015-0662-0>
- [29] Fuentes-Azcatl, R. & Alejandre, J. Non-Polarizable Force Field of Water Based on the Dielectric Constant: TIP4P/ε. *J. Phys. Chem. B*. **118**, 1263-1272 (2014,2)
- [30] Hamidova, R., Kul, I., Safarov, J., Shahverdiyev, A. & Hassel, E. THERMOPHYSICAL PROPERTIES OF 1-BUTYL-3-METHYLIMIDAZOLIUM BIS(TRIFLUOROMETHYLSULFONYL)IMIDE AT HIGH TEMPERATURES AND PRESSURES. *Brazilian Journal Of Chemical Engineering*. **32** (2015,1), <https://doi.org/10.1590/0104-6632.20150321s00003120>
- [31] Gaciño, F., Regueira, T., Comuñas, M., Lugo, L. & Fernández, J. Density and isothermal compressibility for two trialkylimidazolium-based ionic liquids at temperatures from (278 to 398)K and up to 120MPa. *The Journal Of Chemical Thermodynamics*. **81** pp. 124-130 (2015), <https://www.sciencedirect.com/science/article/pii/S0021961414002997>

- [32] Neto, B., Meurer, E., Galaverna, R., Bythell, B., Dupont, J., Cooks, R. & Eberlin, M. Vapors from Ionic Liquids: Reconciling Simulations with Mass Spectrometric Data. *The Journal Of Physical Chemistry Letters*. **3**, 3435-3441 (2012),
- [33] Lemmon EW, McLinden MO, Friend DG (2005) Thermophysical properties of fluid systems, NIST Chemistry WebBook, NIST Standard Reference Database. In: Linstrom PJ, Mallard WG (eds) <http://webbook.nist.gov> (accessed February 1, 2022)
- [34] Martins, M., Neves, C., Kurnia, K., Carvalho, P., Rocha, M., Santos, L., Pinho, S. & Freire, M. Densities, viscosities and derived thermophysical properties of water-saturated imidazolium-based ionic liquids. *Fluid Phase Equilibria*. **407** pp. 188-196 (2016), <https://www.sciencedirect.com/science/article/pii/S0378381215002769>, Aqueous Solutions
- [35] Jacquemin, J., Husson, P., Padua, A. & Majer, V. Density and viscosity of several pure and water-saturated ionic liquids. *Green Chem.* **8**, 172-180 (2006), <http://dx.doi.org/10.1039/B513231B>
- [36] Fuentes-Azcatl, R., Mendoza, N. & Alejandre, J. Improved SPC force field of water based on the dielectric constant: SPC/ $\epsilon$ . *Physica A: Statistical Mechanics And Its Applications*. **420** pp. 116-123 (2015), <https://www.sciencedirect.com/science/article/pii/S0378437114009108>
- [37] Fuentes-Azcatl, R. Flexible model of water based on the dielectric and electromagnetic spectrum properties: TIP4P/ $\epsilon_{Flex}$ . *Journal Of Molecular Liquids*. **338** pp. 116770 (2021), <https://www.sciencedirect.com/science/article/pii/S016773222101494X>
- [38] Fuentes-Azcatl, R. & Barbosa, M. Sodium Chloride, NaCl/ $\epsilon$ : New Force Field. *The Journal Of Physical Chemistry B*. **120**, 2460-2470 (2016,3), <https://doi.org/10.1021/acs.jpcc.5b12584>
- [39] Fuentes-Azcatl, R. & Barbosa, M. Potassium bromide, KBr/ $\epsilon$ : New Force Field. *Physica A: Statistical Mechanics And Its Applications*. **491** pp. 480-489 (2018), <https://www.sciencedirect.com/science/article/pii/S0378437117309731>
- [40] Fuentes-Azcatl, R. & Barbosa, M. Flexible bond and angle, FBA/ $\epsilon$  model of water. *Journal Of Molecular Liquids*. **303** pp. 112598 (2020), <http://www.sciencedirect.com/science/article/pii/S0167732219331496>
- [41] Zaitsau, D., Kabo, G., Strechan, A., Paulechka, Y., Tschersich, A., Verevkin, S. & Heintz, A. Experimental Vapor Pressures of 1-Alkyl-3-methylimidazolium Bis(trifluoromethylsulfonyl)imides and a Correlation Scheme for Estimation of Vaporization Enthalpies of Ionic Liquids. *J. Phys. Chem. A*. **110**, 7303-7306 (2006,6)
- [42] Krossing, I., Slattery, J., Daguene, C., Dyson, P., Oleinikova, A. & Weingärtner, H. Why Are Ionic Liquids Liquid? A Simple Explanation Based on Lattice and Solvation Energies. *J. Am. Chem. Soc.* **128**, 13427-13434 (2006,10)

